

## **Supplemental Materials**

### **Liver-heart crosstalk controls IL-22 activity in cardiac protection after myocardial infarction**

Ting-Ting Tang, Yuan-Yuan Li, Jing-Jing Li, Ke Wang, Yue Han, Wen-Yong Dong, Zheng-Feng Zhu, Ni Xia, Shao-Fang Nie, Min Zhang, Zhi-Peng Zeng, Bing-Jie Lv, Jiao Jiao, Heng Liu, Zong-Shu Xian, Xiang-Ping Yang, Yu Hu, Yu-Hua Liao, Qing Wang, Xin Tu, Ziad Mallat, Yu Huang, Guo-Ping Shi, Xiang Cheng

## **Supplemental Methods**

### **Histological analysis**

At each point, the heart was obtained and cut transversely into three blocks, from the apex to the base. The blocks were fixed in 4% paraformaldehyde at room temperature for 12 hours, embedded in paraffin, and cut into 5- $\mu$ m sections. To assess infarct size and fibrosis, three sections from each of the blocks per heart were stained with Masson's trichrome (Maixin Bio. Co. Ltd., China). Infarct size was measured as the sum of the epicardial and endocardial scar length, divided by the sum of the LV epicardial and endocardial circumferences. To assess fibrosis, we randomly selected five fields (400x magnification) in the peri-infarct zone and calculated the collagen volume fraction as the ratio of the blue-stained (collagen) area to the total tissue area. The collagen-rich border zone of the vessels and the scar were excluded from the analysis. For capillary density analysis, one section from each of the three blocks per heart was stained with anti-CD31 (eBioscience, USA) antibody; the CD31-positive capillaries in 5 randomly selected high visual fields (400x magnification) in the border area were counted.

### **Flow cytometry**

The heart was minced, and digested with a cocktail of type II collagenase, elastase (Worthington Biochemical Corporation, USA) and DNase I (Sigma, USA) as described [1]. Single cell suspensions were obtained by filtering through a 40  $\mu$ m cell strainer (BD Bioscience, USA). Leukocyte-enriched fractions were isolated using 37/70% Percoll (GE Healthcare, USA) and then labeled with surface markers, including APC/Cy7-anti-mouse CD45, PE/CY7-anti-mouse-CD11b, FITC-anti-mouse CD3, PerCP/Cy5.5-anti-mouse CD19, PE-anti- $\gamma\delta$ TCR, Alexa Fluor 488-anti-mouse Ly6G, PE-anti-mouse F4/80, and Alexa Fluor 647-anti-mouse Nkp46. Flow cytometric analyses were performed on a FACSAria machine. Absolute Counting Beads (Invitrogen Life Technologies, USA) were added for absolute cell quantification.

### **Isolation of cardiomyocytes, cardiac fibroblasts, and hepatocytes**

Murine neonatal cardiomyocytes and cardiac fibroblasts were prepared as described [2], with some modifications. Briefly, hearts from 1-day-old C56BL/6 mice were obtained, washed in chilled Dulbecco's modified Eagle's medium (DMEM, Gibco, USA) and cut into 1 mm<sup>3</sup> pieces. The first digestion was discarded, in which the heart pieces were digested with trypsin/EDTA (Gibco, USA) at 4°C for 30 min with rotation. After another 5-6 rounds of digestion with Liberase TH (0.1 U/ml in HBSS, Roche, Germany) at 37°C for 10 min, the cell suspension was collected, filtered through a 70  $\mu$ m cell strainer (BD, USA) and seeded onto fibronectin-coated 12-well tissue culture plates (Costar, USA) in DMEM supplemented with 20% fetal bovine serum (Gibco, USA) and antibiotics (50 mg/ml streptomycin, 50 U/ml penicillin) at 37°C in a 95% O<sub>2</sub> and 5% CO<sub>2</sub> incubator. Cardiac fibroblasts adhere more avidly to plastic than cardiomyocytes.

After 1 hour of incubation, cardiac fibroblasts attached tightly to the plates, whereas the cardiomyocytes-enriched suspension was collected, centrifuged, re-suspended and seeded onto another fibronectin-coated 12-well tissue culture plate. Thereafter, the isolated cardiomyocytes and cardiac fibroblasts were cultured separately for 48-72 hours. A high purity of cardiomyocytes (>90%) and cardiac fibroblasts (>95%) was confirmed using sarcomeric  $\alpha$ -actinin (Boster immunoleader, USA) and vimentin (Sigma, USA) staining, respectively. Primary hepatocytes were isolated as described [3]. Briefly, male C57BL/6 mice aged 6-8 weeks were anesthetized intraperitoneally with 40 mg/kg sodium pentobarbital. After the portal vein was cannulated under aseptic conditions, the liver was perfused with Ethylene glycol bis (2-aminoethyl ether) tetraacetic acid and DMEM (Gibco, USA) and was digested with 0.075% collagenase (Roche, Germany). The isolated mouse hepatocytes were then cultured on mouse-tail collagen-coated plates for 24 hours.

### **Cell lines**

H5V endothelial cells from mouse heart were cultured as described [4].

### **Confocal microscopic assay**

Isolated cardiomyocytes and cardiac fibroblasts were plated onto glass slides, fixed in 4% paraformaldehyde and permeabilized with PBS containing 0.1% Triton X-100. After blocking with goat or mouse serum, double immunofluorescent staining on the slides was performed by incubating the samples with primary rat anti-IL-22R1 (R&D, USA) or anti-IL-10R2 (R&D, USA) and either mouse anti-sarcomeric  $\alpha$ -actinin (Boster immunoleader, USA) or anti-vimentin (Sigma, USA); these antibodies were followed by incubations with secondary Cy3-conjugated anti-rat IgG (Proteintech, USA) and FITC-conjugated anti-mouse IgG (Proteintech, USA). Subsequently, cells were stained with 1  $\mu$ g/ml DAPI to visualize the nuclei and viewed with a microscope.

### **RT-PCR**

Total RNA was extracted from tissues or cultured cells with Trizol (Invitrogen, USA). RNA was reverse transcribed into cDNA using the PrimeScript RT reagent kit (Takara, Japan). The mRNA levels of genes were quantified using SYBR Green Master Mix (Takara, Japan) with the ABI PRISM StepOne™ system (Applied Biosystems, USA). Each reaction was performed in duplicate. The relative mRNA expression of target genes was normalized to  $\beta$ -ACTIN using the  $2^{-\Delta\Delta C_T}$  method. Primer sequences are presented in supplemental Table S8.

### **Western blot**

Total protein extracts were isolated from tissues or cells with lysis buffer (M-PER Mammalian Protein Extraction Reagent, Pierce, USA) containing protease inhibitor cocktail (Roche, Germany). After centrifugation at 16000 g for 10 min at 4 °C, the supernatant was collected, and the total protein concentration was determined using a BCA Protein Assay Kit (Pierce, USA). A total of 30-50  $\mu$ g protein was separated on a SDS-polyacrylamide gel and transferred to a nitrocellulose membrane and probed with antibodies against IL-22R1, IL-10 R2, AGP2 or  $\beta$ -klotho (all from R&D, USA); FGF21 (Aviva, USA); STAT1, phosphate STAT1, STAT3, phosphate STAT3, STAT5, phosphate STAT5, ERK, phosphate ERK, JNK, phosphate JNK, p38, phosphate p38, AKT, phosphate AKT, FGFR1 (all from Cell Signaling Technology, USA);

FGFR2, FGFR3 or FGFR4 (all from Abcam, USA); or  $\beta$ -ACTIN (Santa Cruz Biotechnology, USA).

### **Immunoprecipitation**

Cardiomyocytes were starved for 12 hours, stimulated with FGF21 (1  $\mu$ g/ml, Biovondor, USA) for the indicated times and then lysed. Protein lysates (500  $\mu$ g) were used for immunoprecipitation using the Pierce™ Crosslink IP kit (Thermo, USA). Briefly, protein lysates were immunoprecipitated using pre-cross-linked anti-FGFR1/2/3/4 antibody and protein A/G-Sepharose beads at 4°C overnight. The immunoprecipitates were washed with lysis buffer, eluted with Laemmli sample buffer and then subjected to immunoblotting analysis using anti-phosphotyrosine (Abcam, USA).

### **Microarray analysis**

Total RNA was extracted from cardiomyocytes after exposure to hypoxia (in 2% oxygen, 5% CO<sub>2</sub> and 93% N<sub>2</sub>) for 12 hours with or without FGF21 (1  $\mu$ g/ml) using Trizol (Invitrogen, USA). Samples were processed for hybridization to the Mouse Gene 2.0 ST Array (Affymetrix). Prior to data analysis, all arrays referred to in this study were assessed for data quality using the Affymetrix Expression Console software v.1.3, and all quality assessment metrics (including spike-in controls during target preparation and hybridization) were found within boundaries. Genes showing 1.5 or greater fold changes with an adjusted value of  $p < 0.05$  are considered as differentially expressed. The data set has been deposited in Gene Expression Omnibus (GEO, <http://www.ncbi.nlm.nih.gov/geo/>) under accession number GSE80199. Microarray data were also examined by gene set enrichment analysis (GSEA, <http://software.broadinstitute.org/gsea/index.jsp>) using the HALLMARK gene sets.

### **ELISA**

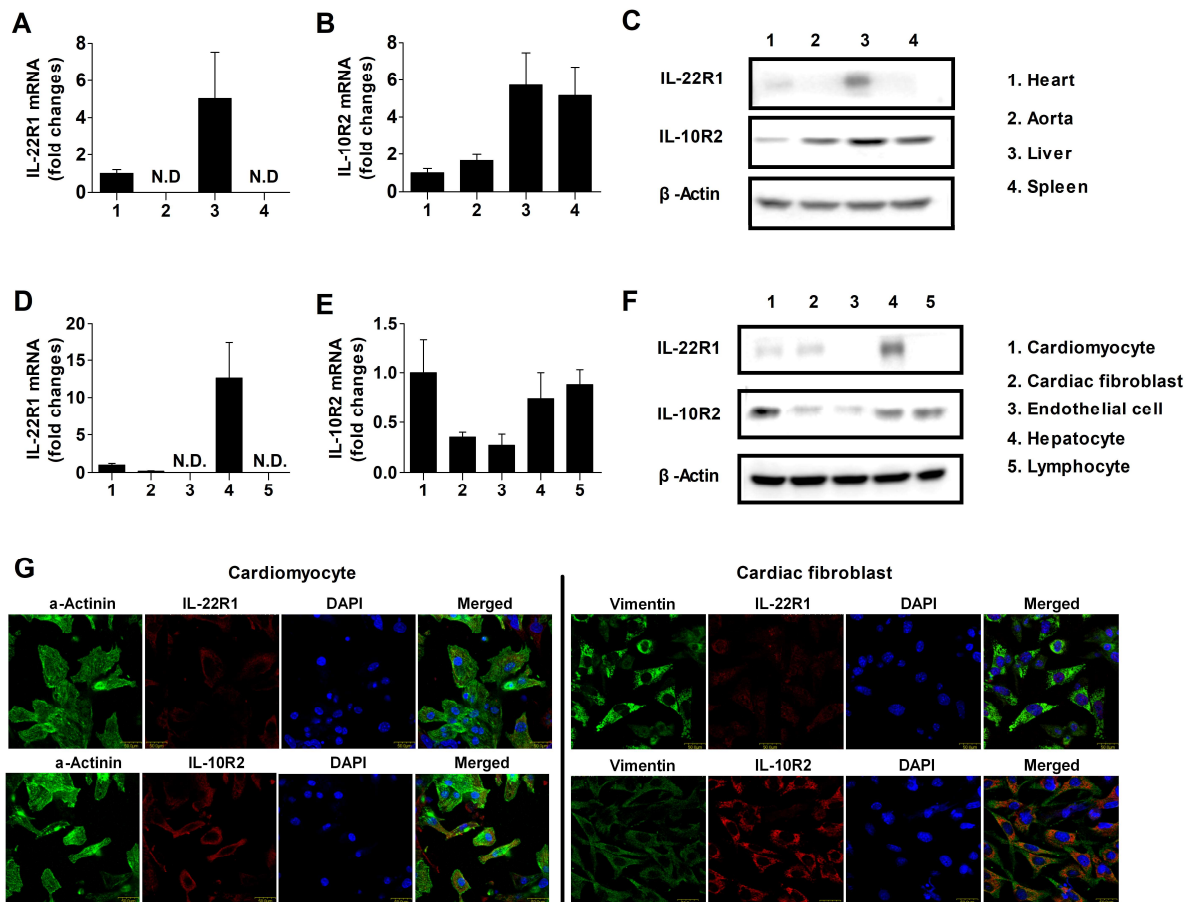
Mouse IL-22 (BioLegend, USA), FGF21 (R&D, USA), and STAT3 (RayBiotech, USA) ELISA were performed according to the manufacturer's instructions.

### **Caspase-3 activity assay**

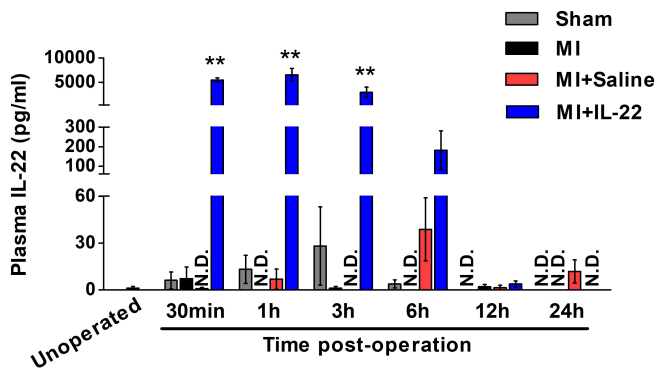
Caspase-3 activity was determined by the Caspase-3 activity assay kit (Beyotime, China) according to the manufacturer's instructions.

### **References**

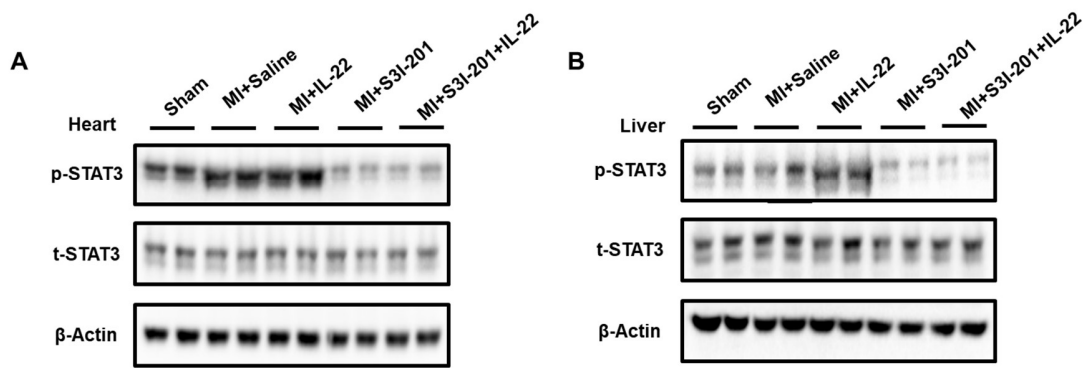
1. Yan X, Anzai A, Katsumata Y, et al. Temporal dynamics of cardiac immune cell accumulation following acute myocardial infarction. *J Mol Cell Cardiol.* 2013; 62:24-35.
2. Rui T, Cepinskas G, Feng Q, Ho YS, Kvietys PR. Cardiac myocytes exposed to anoxia-reoxygenation promote neutrophil transendothelial migration. *Am J Physiol Heart Circ Physiol.* 2001; 281:H440-447.
3. Kim WH, Hong F, Jaruga B, et al. Additive activation of hepatic NF-kappaB by ethanol and hepatitis B protein X (HBX) or HCV core protein: involvement of TNF-alpha receptor 1-independent and -dependent mechanisms. *FASEB J.* 2001; 15: 2551- 2553.
4. Cheng KT, Leung YK, Shen B, et al. CNGA2 channels mediate adenosine-induced Ca<sup>2+</sup> influx in vascular endothelial cells. *Arterioscler Thromb Vasc Biol.* 2008; 28:913-918.



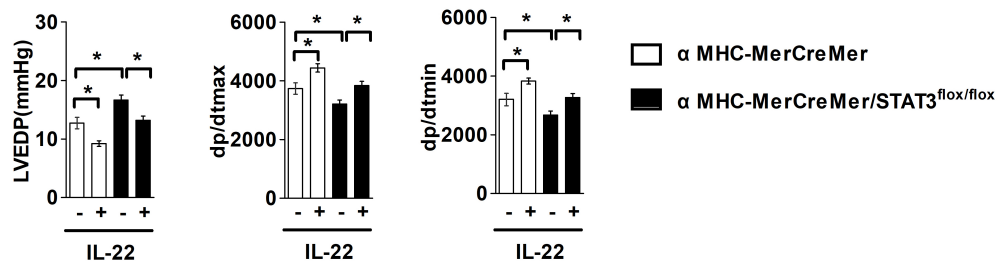
**Supplemental Figure S1** IL-22R1 and IL-10R2 expression in the heart and heart resident cells. RT-PCR (A, B) and immunoblot analysis (C) determined the expression of IL-22R1 and IL-10R2 in the mouse heart, aorta, liver, and spleen. RT-PCR (D, E) and immunoblot analysis (F) determined the expression of IL-22R1 and IL-10R2 in cardiomyocytes, cardiac fibroblasts, cardiac microvascular endothelial cells (H5V), primary hepatocytes, and lymphocytes. (G) Representative confocal microscopy images of IL-22 R1 and IL-10R2 in cardiomyocytes and cardiac fibroblasts. Data represent at least three independent experiments. N.D.: not detectable.



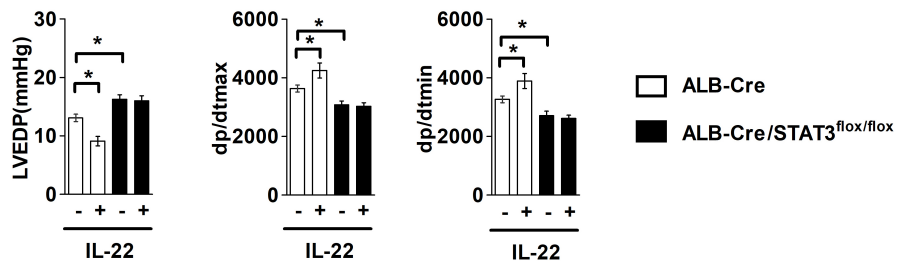
**Supplemental Figure S2** IL-22 administration dramatically increases plasma IL-22 levels. Plasma IL-22 levels were determined in unoperated mice and mice from Sham, MI, MI+Saline and MI+IL-22 groups at different time points after the operation. n=5 per group. N.D.: not detectable. \*\* $p < 0.01$  vs. MI+Saline group by one-way ANOVA.



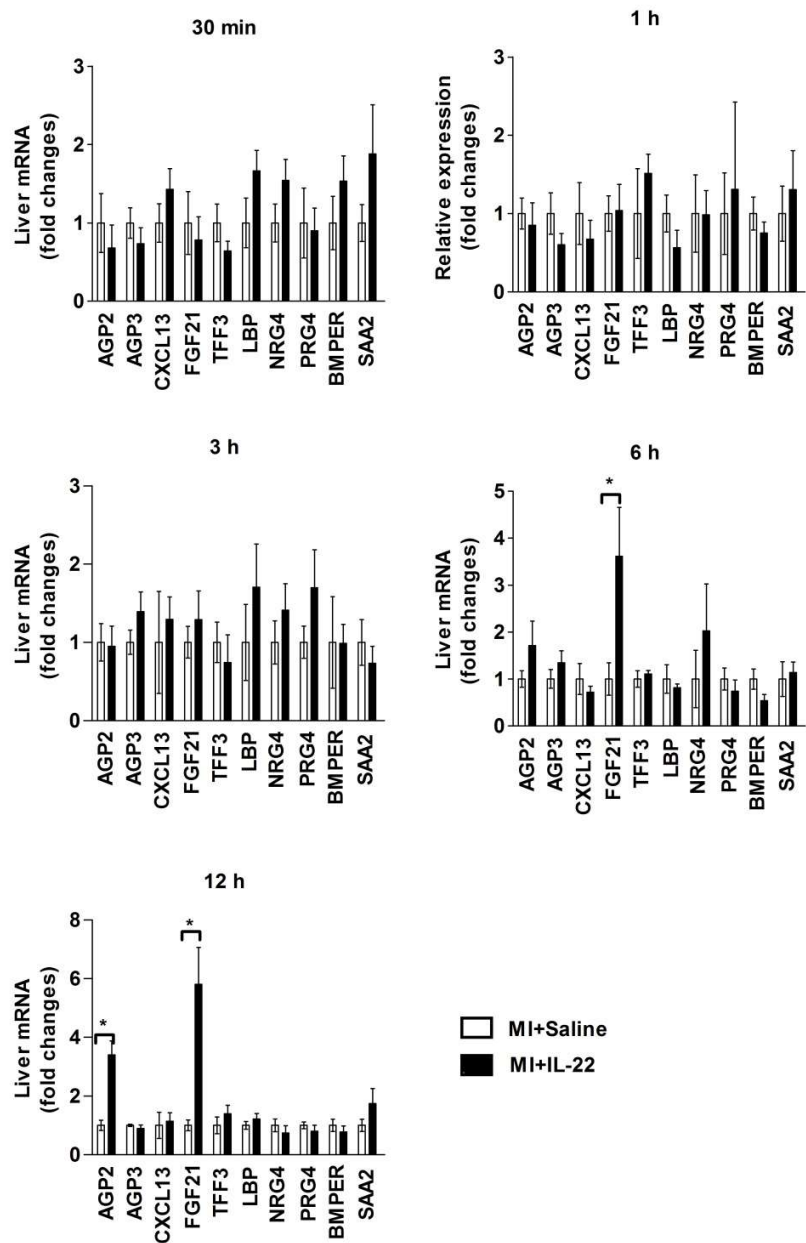
**Supplemental Figure S3** S3I-201 effectively inhibited phosphorylation of STAT3 *in vivo*. S3I-201 was administered intraperitoneally at a dose of 5 mg/kg 1 day prior to sham operation or coronary artery ligation. IL-22 was administered subcutaneously at a dose of 100 µg/kg immediately after the operation. STAT3 phosphorylation in the heart (A) and liver (B) was determined 1 hour after the operation by western blot. Data represent three independent experiments.



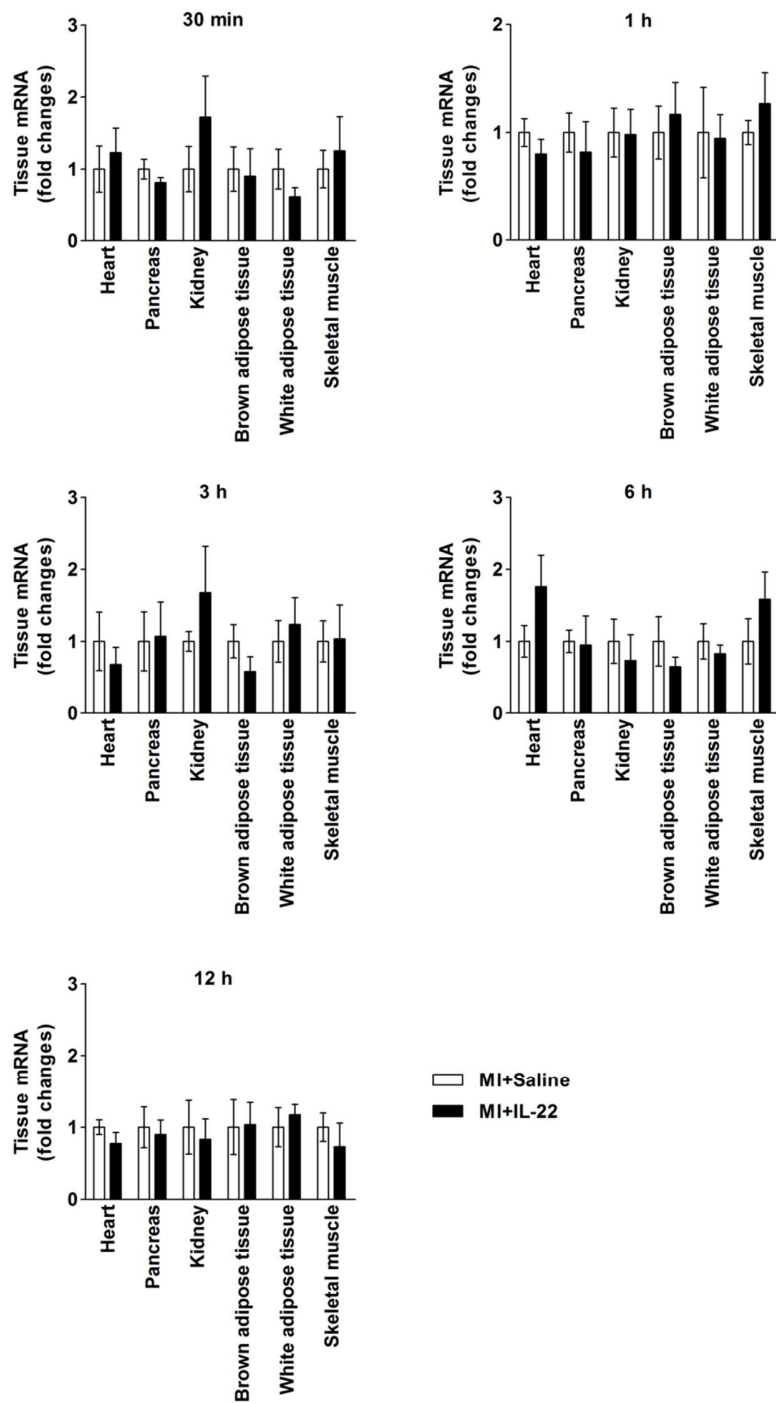
**Supplemental Figure S4** IL-22 improved cardiac function in cardiac-specific STAT3 KO mice. Quantification of LVEDP, dp/dtmax, and dp/dtmin by hemodynamic analysis at 28 days after the operation. n=10 per group. \* $p < 0.05$  by one-way ANOVA.



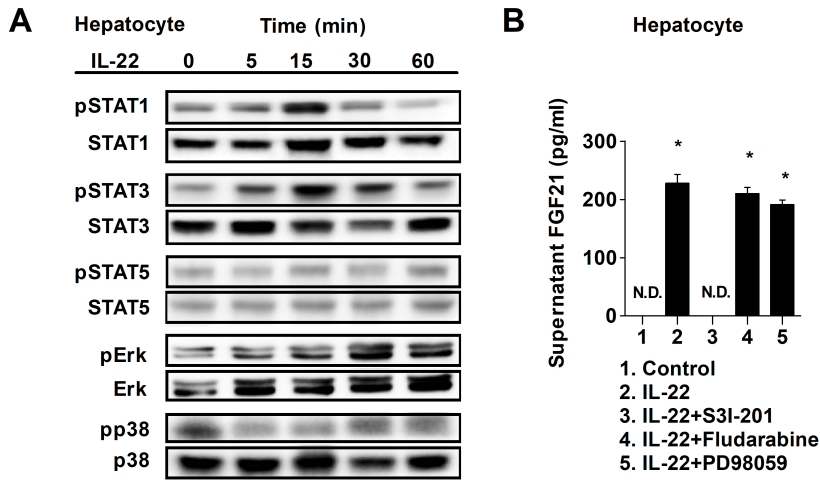
**Supplemental Figure S5** IL-22 failed to improve cardiac function in hepatic-specific STAT3 KO mice. Quantification of LVEDP, dp/dtmax, and dp/dtmin by hemodynamic analysis at 28 days after the operation. n=10 per group. \* $p < 0.05$  by one-way ANOVA.



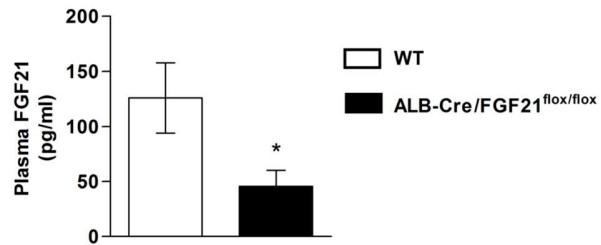
**Supplemental Figure S6** IL-22 increases liver FGF21 and AGP2 expression. RT-PCR determined the mRNA levels of AGP2, AGP3, CXCL13, FGF21, TFF3, LBP, NRG4, PRG4, BMPER and SAA2 in the liver at different time points post-MI between IL-22- and saline-treated mice.  $n=5$  per group.  $*p < 0.05$  vs. MI+saline group by unpaired  $t$  test.



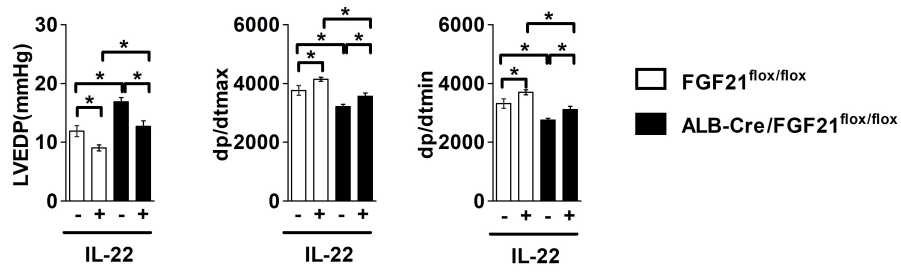
**Supplemental Figure S7** IL-22 does not induce FGF21 expression in other tested organs and tissues besides liver. Relative mRNA FGF21 levels in heart, pancreas, kidney, brown/white adipose tissues, and skeletal muscle at different time points post-MI between IL-22 and saline-treated mice. n=5 per group.



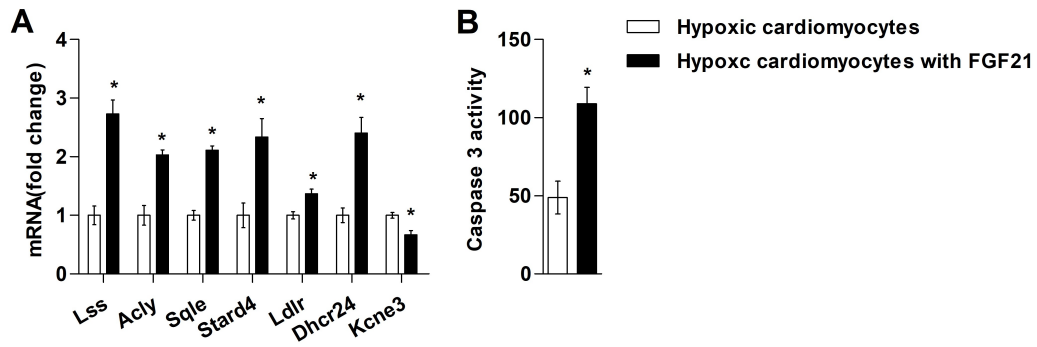
**Supplemental Figure S8** IL-22 stimulates cultured hepatocytes to produce FGF21 by activating STAT3. (A) Representative western blot images of STAT1/3/5, Erk and p38 in hepatocytes following IL-22 stimulation. Data represent at least three independent experiments. (B) ELISA determined supernatant concentration of FGF21 in cultured hepatocytes stimulated without or with IL-22, IL22+S3I-201 (STAT3 inhibitor), IL22+fludarabine (STAT1 inhibitor), or IL-22+PD98059 (Erk inhibitor). \* $p < 0.05$  vs. control by one-way ANOVA.



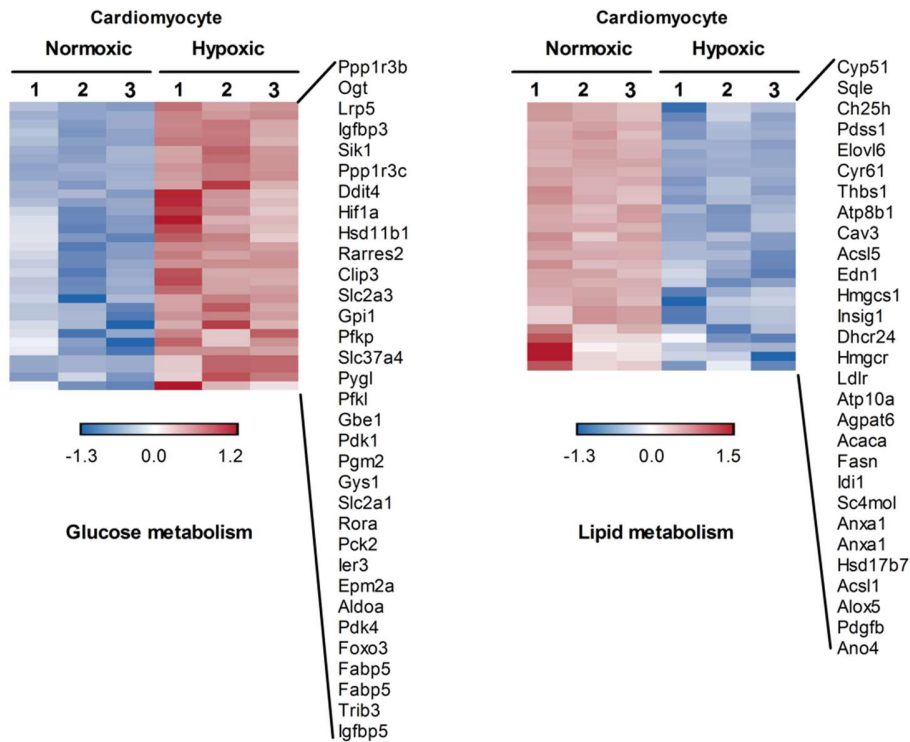
**Supplemental Figure S9** Plasma FGF21 levels are decreased in liver-specific FGF21 KO mice. ELISA determined plasma FGF21 levels in WT and ALB-Cre/FGF21<sup>flox/flox</sup> mice under basal condition. n=8 per group. \* $p < 0.05$  vs. WT group by unpaired  $t$  test.



**Supplemental FigureS10** IL-22 improved cardiac function in hepatic-specific FGF21 KO mice. Quantification of LVEDP, dp/dtmax, and dp/dtmin by hemodynamic analysis at 28 days after operation. n=10 per group. \* $p < 0.05$  by one-way ANOVA.



**Supplemental FigureS11** (A) Microarray data were validated with RT-PCR. (B) Caspase-3 activities were compared in hypoxic cardiomyocytes in the absence or presence of FGF21. \* $p < 0.05$  vs. hypoxic cardiomyocytes by unpaired  $t$  test.



**Supplemental Figure S12** Microarray analysis of cardiomyocytes under hypoxic and normoxic conditions. Heat maps show differentially regulated genes involved in glucose metabolism (left panel) and lipid metabolism (right panel) in cardiomyocytes. Red represents up-regulation and blue represents down-regulation.

**Supplemental Table S1** Echocardiographic measurements in wild type mice

Parameters	LVEDD (mm)	LVESD (mm)	FS (%)	EF (%)
Sham	3.45±0.11	2.08±0.12	40.22±1.93	71.51±2.22
MI	4.60±0.20*	3.88±0.21*	16.06±1.07*	33.78±2.07*
MI+Saline	4.58±0.15*	3.88±0.14*	15.39±0.73*	32.57±1.43*
MI+IL-22	4.01±0.04*#	3.14±0.04*#	21.75±0.78*#	44.43±1.35*#

n=10-15 in each group. LVEDD indicates left ventricular end-diastolic diameter; LVESD, left ventricular end-systolic diameter; FS, fractional shortening; EF, ejection fraction. \* $p$ <0.05 vs. Sham group. # $p$ <0.05 vs. MI+Saline group.

**Supplemental Table S2** Echocardiographic measurements in wild type mice

Parameters	LVEDD (mm)	LVESD (mm)	FS (%)	EF (%)
Sham	3.60±0.08	2.16±0.07	40.01±1.28	71.43±1.62
MI+Saline	4.64±0.05*	3.81±0.07*	17.88±0.78*	37.18±1.44*
MI+IL-22	4.07±0.07*#	3.11±0.09*#	23.67±1.49*#	47.46±2.42*#
MI+S3I-201	5.13±0.18*#	4.45±0.14*#	13.22±0.65*#	28.13±1.22*#
MI+S3I-201+IL-22	5.03±0.11*#	4.35±0.10*#	13.38±0.66*#	28.50±1.27*#

n=8-10 in each group. LVEDD indicates left ventricular end-diastolic diameter; LVESD, left ventricular end-systolic diameter; FS, fractional shortening; EF, ejection fraction. \* $p$ <0.05 vs. Sham group. # $p$ <0.05 vs. MI+Saline group.

**Supplemental Table S3** Echocardiographic measurements in cardiac-specific STAT3 KO mice and control mice

Parameters	LVEDD (mm)	LVESD (mm)	FS (%)	EF (%)
αMHC-MerCreMer+Saline	4.54±0.15	3.77±0.13	16.80±0.65	35.27±1.20
αMHC-MerCreMer+IL-22	4.00±0.12*	3.11±0.09*	22.22±1.09*	45.23±1.84*
αMHC-MerCreMer/STAT3 <sup>flx/flx</sup> +Saline	5.14±0.15*	4.44±0.12*	13.71±0.38*	29.11±0.70*
αMHC-MerCreMer/STAT3 <sup>flx/flx</sup> +IL-22	4.46±0.11#	3.62±0.07#	18.68±1.19#	38.64±2.06#

n=8 in each group. LVEDD indicates left ventricular end-diastolic diameter; LVESD, left ventricular end-systolic diameter; FS, fractional shortening; EF, ejection fraction. \* $p$ <0.05 vs. αMHC-MerCreMer+Saline group. # $p$ <0.05 vs. αMHC-MerCreMer/STAT3<sup>flx/flx</sup>+Saline group.

**Supplemental Table S4** Echocardiographic measurements in hepatic-specific STAT3 KO mice and control mice

Parameters	LVEDD (mm)	LVESD (mm)	FS (%)	EF (%)
ALB-Cre+Saline	4.72±0.07	3.84±0.07	18.60±1.09	38.46±1.78
ALB-Cre +IL-22	4.19±0.14*	3.23±0.10*	22.74±1.51*	45.87±2.16*
ALB-Cre /STAT3 <sup>flx/flx</sup> +Saline	5.34±0.09*	4.57±0.05*	14.37±0.89*	30.51±1.50*
ALB-Cre /STAT3 <sup>flx/flx</sup> +IL-22	5.19±0.13	4.40±0.09	15.22±1.20	31.87±2.00

n=8 in each group. LVEDD indicates left ventricular end-diastolic diameter; LVESD, left ventricular end-systolic diameter; FS, fractional shortening; EF, ejection fraction. \* $p < 0.05$  vs ALB-Cre+Saline group.

**Supplemental Table S5** Echocardiographic measurements in hepatic-specific FGF21 KO mice and control mice

Parameters	LVEDD (mm)	LVESD (mm)	FS (%)	EF (%)
FGF21 <sup>flox/flox</sup> +Saline	4.49±0.11	3.71±0.11	17.35±1.28	36.19±2.31
FGF21 <sup>flox/flox</sup> +IL-22	3.89±0.20*	2.95±0.15*	24.20±1.15*	48.67±1.88*
ALB-Cre /FGF21 <sup>flox/flox</sup> +Saline	5.14±0.07*	4.42±0.05*	13.98±0.64*	29.05±1.60*
ALB-Cre /FGF21 <sup>flox/flox</sup> +IL-22	4.57±0.08#&	3.78±0.07#&	17.16±0.62#&	35.84±1.73#&

n=8-12 in each group. LVEDD indicates left ventricular end-diastolic diameter; LVESD, left ventricular end-systolic diameter; FS, fractional shortening; EF, ejection fraction. \* $p < 0.05$  vs FGF21<sup>flox/flox</sup> +Saline group. # $p < 0.05$  vs. ALB-Cre /FGF21<sup>flox/flox</sup> +Saline group. &  $p < 0.05$  vs FGF21<sup>flox/flox</sup> +IL-22 group.

**Supplemental Table S6** Differentially expressed genes from microarray analysis (Fold change  $\geq 1.5$  or  $\leq -1.5$  and  $p \leq 0.05$ ) in hypoxic cardiomyocytes with vs. without FGF21

Probe Set ID	Symbol	Name	Fold change	Function
<b>Lipid Metabolism</b>				
17234552	LSS	Lanosterol synthase	1.74	cholesterol biosynthesis
17269521	ACLY	ATP-citrate synthase	1.53	de novo lipid synthesis and glucose/energy metabolism
17273348	FASN	Fatty acid synthase	1.52	long-chain fatty acids synthesis, energy reserve metabolic process
17285056	IDI1	Isopentenyl-diphosphate delta isomerase	2.13	cholesterol biosynthesis and metabolism
17290173	HMGCS1	3-Hydroxy-3-methylglutaryl-CoA synthase 1	1.69	cholesterol biosynthesis and metabolism
17295233	HMGCR	3-Hydroxy-3-methylglutaryl-CoA reductase	1.54	cholesterol biosynthesis and metabolism
17307588	FDFT1	Farnesyl-diphosphate farnesyltransferase 1	1.74	oxidoreductase activity and squalene synthase activity
17311807	SQLE	Squalene epoxidase	1.81	flavin adenine dinucleotide binding and squalene monooxygenase activity
17353358	STARD4	StAR-related lipid transfer (START) domain containing 4	1.58	lipid binding
17362595	FADS2	Fatty acid desaturase 2	1.64	iron ion binding and stearoyl-CoA 9-desaturase activity
17402558	ELOVL6	ELOVL fatty acid elongase 6	1.83	cholesterol biosynthesis and metabolism
17406908	FDPS	Farnesyl diphosphate synthase	1.89	isoprenoid biosynthesis
17435584	INSIG1	Insulin induced gene 1	1.74	cholesterol biosynthesis and metabolism

17445308	CYP51	Cytochrome P450, family 51, subfamily A, oolypeptide 1	2.12	cholesterol biosynthesis and metabolism, and electron carrier activity and heme binding
17509629	SC4MOL	Methylsterol monooxygenase 1	1.97	iron ion binding and C-4 methylsterol oxidase activity cholesterol biosynthesis
17515315	LDLR	Low density lipoprotein receptor	1.55	calcium ion binding and low-density lipoprotein particle binding
17535434	NSDHL	NAD(P) dependent steroid dehydrogenase-like	1.77	cholesterol biosynthesis

### Cell proliferation, death and apoptosis

17416325	DHCR24	24-Dehydrocholesterol reductase	1.74	protect cells from oxidative stress by reducing caspase 3 activity during apoptosis protects against amyloid-beta peptide-induced apoptosis. cell death and cell proliferation
17548559	EMP1	Epithelial membrane protein 1	1.62	cell cycle
17547744	CKS2	CDC28 protein kinase regulatory subunit 2	1.52	mitotic and cell cycle
17344990	CENPQ	Centromere protein Q	1.51	

### Ion homeostasis

17450387	SPARCL1	SPARC-like 1 (hevin)	-1.54	calcium ion binding
17472530	KCNJ8	Potassium channel, inwardly rectifying subfamily J, member 8	-1.57	inward rectifier potassium channel activity and ATP-activated inward rectifier potassium channel activity
1748064	KCNE3	Potassium channel, voltage gated subfamily E regulatory beta subunit 3	-1.54	voltage-gated potassium channel activity and potassium channel regulator activity

### Others

17466919	HIBADH	3-Hydroxyisobutyrate dehydrogenase	1.50	catabolism of L-valine
17375454	SLC28a2	Solute carrier family 28	1.50	nucleoside binding and purine nucleoside transmembrane transporter activity
17324835	TFRC	Transferrin receptor	1.58	endocytosis
17346062	ZFP119a	Zinc finger protein 119a	1.63	regulation of transcription
17234423	DERL3	Derlin 3	-1.63	degradation of misfolded glycoproteins in the endoplasmic reticulum
17337770	GPR116	Adhesion G protein-coupled receptor F5	-1.51	regulation of acid-base balance
17448924	KDR	Kinase insert domain receptor	-1.53	protein tyrosine kinase activity and transmembrane receptor protein tyrosine kinase activity
17228792	-	-	1.81	unknown
17231759	Gm10335	-	1.54	unknown
17262241	-	-	1.55	unknown
17267418	A130040M12Rik	-	1.50	unknown
17377459	-	-	1.66	unknown
17395398	C330013J21Rik	-	1.67	unknown

17462661	Gm8430	-	1.74	unknown
17504019	-	-	1.61	unknown
17516613	-	-	1.51	unknown
17548955	Gm12891	-	1.52	unknown
17419058		-	-1.54	unknown
17465731		-	-1.71	unknown
17513399		-	-1.55	unknown
17540366		-	-1.52	unknown
17544358		-	-1.51	unknown

---

**Supplemental Table S7** GSEA of hypoxic cardiomyocytes with vs. without FGF21

Gene Set Name	NES	FDR q-val
HALLMARK_CHOLESTEROL_HOMEOSTASIS	2.854655	0
HALLMARK_G2M_CHECKPOINT	2.732635	0
HALLMARK_E2F_TARGETS	2.682186	0
HALLMARK_MTORC1_SIGNALING	2.401328	0
HALLMARK_MYC_TARGETS_V1	2.355443	0
HALLMARK_MITOTIC_SPINDLE	2.343917	0
HALLMARK_DNA_REPAIR	2.013368	0
HALLMARK_MYC_TARGETS_V2	1.943671	1.55E-04
HALLMARK_ANDROGEN_RESPONSE	1.936823	1.38E-04
HALLMARK_FATTY_ACID_METABOLISM	1.740063	0.001624775
HALLMARK_PEROXISOME	1.737276	0.001602942
HALLMARK_UV_RESPONSE_DN	1.592977	0.00946627
HALLMARK_TNFA_SIGNALING_VIA_NFKB	1.539828	0.015261021
HALLMARK_OXIDATIVE_PHOSPHORYLATION	1.427568	0.045106538
HALLMARK_PROTEIN_SECRETION	1.417744	0.046820093
HALLMARK_GLYCOLYSIS	1.412448	0.046811488
HALLMARK_APOPTOSIS	1.324326	0.09854584
HALLMARK_UV_RESPONSE_UP	1.319057	0.0976579
HALLMARK_ESTROGEN_RESPONSE_EARLY	1.31192	0.099230565
HALLMARK_ESTROGEN_RESPONSE_LATE	1.2188	0.20270298

NES, normalized enrichment score; FDR, false discovery rate.

**Supplemental Table S8** Primer sequences

Genes	Primer pairs, 5'→3'	Genes	Primer pairs, 5'→3'
IL-22R1	F- ctacgtgtgccgagtgaaga R- aagcgtaggggtgaaaggt	LSS	F-tttaggctgtagcaggtcat R-caggctccaacttcattt
IL-10R2	F-tggagtgaaacctctgtga R-agcagaaacgtcctgtgatg	ACLY	F-aagagggattacagtgatgg R-aaagatgctgcctactgggt
FGF21	F-ggtcattcaaatcctgggtg R-ctggttggggagtccttct	FASN	F-tggcttccaactcctactca R-cagggctcaccaggtgtt
AGP2	F-actggaaaaggacaggtgca R-cagccctcggagttcagaga	IDI1	F-tccaccttctctgactc R-cctactcctcccacttc
AGP3	F-ttctcattgtgtggtgac R-gcactctcaggtggagaagg	HMGCS1	F-cttctttgtctcgttctt R-tttccagcatctacacat
CXCL13	F-catcatgaggtggtgcaaag R-gggtcacagtgcaaaggaat	HMGCR	F-tgttcacgctcatagtcgc R-gaaggctaaactcagggtaat
TFF3	F-taatgtgtgtggtgctctg R-cagccaaggtgttacactg	FDFT1	F-caaaggcaccaccgaact R-aactccaagcgggacagc
NRG4	F-cagaccaagatccagcaca R-aataaccagttccgcacagg	SQLE	F-gaggaaggcaagtgtcgg R-gatctgggtgctgggaaa
FGL1	F-gtggggctagtcaccaaaagga R-ttctgcctgtaggaaccac	STARD4	F-tgtttcccttctcctcgt R-cagaccttctgcctttg
FGL2	F-attagatgtgaaccggctgtga R-tggcaaatctaaccgtgtgg	FADS2	F-gaagctgaaataacctgcctac R-gctcccaagatgccgtaga
SAA2	F-tgtctctgtcctctctg R-ctggctggaagatggagac	ELOVL6	F-gcctacatcggcaaaagt R-cctctgctcctcctacac
LBP	F-ggctgctgaatctctccac R-gagcgggtgattccgattaaa	FDPS	F-ggtggagccgaagaaaca R-cagcaaacgatagatggagg

FGFR1	F-atggttgaccgttctggaag R-tggaagtcgctcttcttggt	INSIG1	F-gatagccaccatcttctcct R-aacgaacacggcaataca
FGFR2	F-caccaactgcaccaatgaac R-gaatcgtcccctgaagaaca	CYP51	F-ctggcgctcatcgttggtg R-ctggccttcttctctctctc
FGFR3	F-catccggcagacatacacac R-ttcaactccacgtgcttcag	SC4MOL	F-aggaggctgaagttgacg R-aaaccagaccagagcag
FGFR4	F-ggggagcagcaatgftgtat R-caaaacagggccagagagag	LDLR	F-cttctcgcctgactctgc R-atggcgacttgggcttgt
NSDHL	F-cagtgtctgcctctatgttt R-cagccatcatctctgttta	DHCR24	F-aaagcctcgtgttgaagcc R-gccgcatcagtgagcacc
EMP1	F-ttcaactaggagcataactgg R-gcaatggtggagacaac	CKS2	F-tcctgateccgcttactc R-ctctccactcctctctcg
CENPQ	F-ttgaaacaaagaccaataagg R-ggaagaggtgccagggt	SPARCL1	F-gaccactccaaccaacta R-ctccatcctcctcatcctt
KCNJ8	F-aagtgaccattgggttcgg R-ggacggcaatcacagcat	KCNE3	F-ctggtaagagggttaggtca R-cttctactgtctggtgtcc
HIBADH	F-ccagcgacacttacaacc R-ctttctttgagtagcccttt	SLC28a2	F-aatggagccacagatgcc R-ggagcagatgacctggaaa
TFRC	F-cctgtcgccctatgtatc R-ctccctgaatagtccaagt	ZFP119a	F-tgggacaaagaaagtgg R-aagatacctgggatgggt
DERL3	F-ccctgggattcggcttct R-ctcgcgacggctccaatac	GPR116	F-ggaataccgtaagcatcacc R-ccactcacctgcaataac
β-ACTIN	F- aaggccaaccgtgaaaagat R- gtggtacgaccagaggcatac	KDR	F-gctgtgaacccttgccttat R-caacatcttgacggctactg

---